PATIENT SPECIFIC MUSCULOSKELETAL MODELING TO RELATE INTRA OPERATIVE MUSCLE FORCE DATA TO GAIT IN CEREBRAL PALSY

by

Utku Can

B.S., in Mechanical Engineering, Boğaziçi University, 2014

Submitted to the Institute of Biomedical Engineering
in partial fulfillment of the requirements
for the degree of
Master of Science
in
Biomedical Engineering

Boğaziçi University
2019

PATIENT SPECIFIC MUSCULOSKELETAL MODELING TO RELATE INTRA OPERATIVE MUSCLE FORCE DATA TO GAIT IN CEREBRAL PALSY

APPROVED BY:

Prof. Dr. Can Yücesoy .....
(Thesis Advisor)

Assoc. Prof. Dr. Fuat Bilgili .....

Assoc. Prof. Dr. Evren Samur .....

DATE OF APPROVAL: 5 September 2019

ACKNOWLEDGMENTS

First, I would like to thank my thesis supervisor, Prof. Dr. Can Yücesoy, for all his guidance, valuable comments and continuous support. I could not be more thankful and know that cannot complete my study without his mentorship. I am going to use his precious advices in not only my academic life, but also in my professional career and private life as well.

I also want to thank Cemre Su Kaya, for the intra-operative muscle force data and her support whenever I need. She always had time for me when I looked for a contribution to my study. I wish all the best for her in the future.

I want to thank Assoc. Prof. Dr. Fuat Bilgili and Assoc. Prof. Dr. Evren Samur for participating and contributing my thesis defense.

At most, I want to thank my beloved Fulya Başağaç. Nothing could be achievable for me without her endless support, encouragement and belief in me. I would love to dedicate my study and my degree to her, for making it real.

This study is supported by TUBITAK with the project name 'Assessment of mechanics of spastic muscle with intraoperative experiments: developing novel approaches to show that limited joint motion is caused by an integral abnormal functioning of the muscle-connective tissue system (TUBITAK Research Fund, grant no:113S293)'.

ACADEMIC ETHICS AND INTEGRITY STATEMENT

I, Utku Can, hereby certify that I am aware of the Academic Ethics and Integrity Policy issued by the Council of Higher Education (YÖK) and I fully acknowledge all the consequences due to its violation by plagiarism or any other way.

Name :

Signature:

Date:

ABSTRACT

PATIENT SPECIFIC MUSCULOSKELETAL MODELING TO RELATE INTRA OPERATIVE MUSCLE FORCE DATA TO GAIT IN CEREBRAL PALSY

Increased pathological resistance against knee extension is a characteristic pathological condition in cerebral palsy (CP). Active and passive forces of spastic knee flexor muscles have been associated with the high forces which constrain the knee movement in flexed positions. However, studies quantifying these forces directly are rare. The aim of this study was to determine (1) if the range for spastic muscle-tendon complex length is comparable to that of healthy muscle and (2) how spastic muscle force changes as a function of muscle-tendon complex length. Musculoskeletal patient specific models were developed using OpenSim software by using the gait analysis data of CP patients. The results suggest that the muscle-tendon complex length trends of the patients are similar to those of healthy individuals. The difference between the minimum and maximum MTL is 13% and 8% for healthy ST-GRA muscles respectively, while this difference oscillates between 7% and 14% for spastic ST muscles and 4%-9% for spastic GRA muscles of the patients. In addition, at longer muscle-tendon complex lengths higher passive and active forces of spastic muscles were measured and the dominant component of the total force is the active muscle force. For the GRA, peak active muscle force is more than 5 times that of passive force. For the ST, peak active muscle force is approximately 4 times that of passive force. The outcome of this assessment suggests that mechanical characteristics of spastic muscles may not necessarily differ from those of healthy muscles. This implies that, an explanation for the restricted joint movement of CP patients via the consideration of spastic muscles as shortened and mechanically abnormal muscles is a simplistic one.

Keywords: Cerebral palsy; Musculoskeletal system model; Spastic muscle mechanics.

ÖZET

SEREBRAL PALSİDE İNTRAOPERATİF KAS KUVVET DATASI İLE YÜRÜYÜŞ BİÇİMİNİ İLİŞKİLENDİRMEK İÇİN HASTAYA ÖZGÜ İSKELET KAS MODELLEMESİ

Diz ekstansiyonuna karşı artan patolojik direnç, serebral palside (CP) karakteristik bir patolojik durumdur. Spastik diz fleksör kaslarının aktif ve pasif kuvvetleri, diz hareketini bükülmüş pozisyonlarda tutan yüksek kuvvetlerle ilişkilendirilmiştir. Ancak, bu kuvvetleri doğrudan ölçen çalışmalar nadirdir. Bu çalışmanın amacı (1) spastik kas-tendon kompleksi uzunluğu aralığının sağlıklı kas ile karşılaştırılabilir olup olmadığını ve (2) spastik kas kuvvetinin kas-tendon kompleksi uzunluğunun fonksiyonu olarak nasıl değiştiğini tespit etmektir. Hastalara özgü iskelet kas sistemi modelleri, CP hastalarının yürüyüş analizi verileri kullanılarak OpenSim yazılımı ile geliştirilmiştir. Sonuçlar, hastaların kas-tendon kompleks uzunluğu eğilimlerinin sağlıklı bireylerinkine benzer olduğunu göstermektedir. Minimum ve maksimum MTL arasındaki fark, sağlıklı ST-GRA kasları için sırasıyla %13 ve %8'dir. Bu fark spastik ST kasları için %7 ila %14, ve spastik GRA kasları için %4 ile %9 arasında salınmaktadır. Ek olarak, daha uzun kas-tendon kompleks uzunluklarında daha yüksek pasif ve aktif spastik kas kuvvetleri ölçülmüş, ve toplam kuvvetin baskın bileşenini aktif kas kuvveti oluşturmuştur. GRA için pik aktif kas kuvveti, pasif kuvvetin 5 katından fazladır. ST için, aktif aktif kas kuvveti, pasif kuvvetin yaklaşık 4 katıdır. Bu değerlendirmenin sonucu, spastik kasların mekanik özelliklerinin, sağlıklı kasların özelliklerinden farklı olmak zorunda olmadığıdır. Bu, spastik kasların kısalmış ve mekanik olarak anormal kaslar olarak değerlendirilmesiyle CP hastalarının kısıtlı eklem hareketleri için yapılan açıklamaların basite indirgenmiş olabileceği anlamına gelir.

Anahtar Sözcükler: Serebral palsi; Kas-iskelet sistemi modeli; Spastik kas mekaniği.

TABLE OF CONTENTS

LIST OF FIGURES

LIST OF TABLES

LIST OF ABBREVIATIONS

ST	Semitendinosus
GRA	Gracilis
HA	Hip Angle
KA	Knee Angle
MTL	Muscle-Tendon Complex Length
TD	Typically Developed

1. INTRODUCTION

1.1 Cerebral Palsy

Cerebral palsy is a neuromuscular system related disease causing disorder of movement, muscle tone or posture. It basically originates from the damage on an immature and developing brain, most of the time before the birth. Mainly, impaired movement in relation to the improper reflexes, floppiness or the rigidity of the limbs. In addition to that, it also causes inappropriate posture along with abnormal waling and involuntarily movements or a combination of these. Exaggerated stretch reflexes triggered by reduced inhibition can be related to these deformities in which the main countenance is skeletal muscle spasticity [1],[2]. Accordingly, the spastic muscle resists lengthening actively and stands at a relatively lower length, provided that it is tried to be stretched quickly. Because of this phenomenon, some structural changes mostly occur after the shortened status of skeletal muscle, where the opposition against stretching remains long lasting [3],[4].

Equines disorder at the ankles and/or flexion of the hips and knees are observed in the lower extremities of the suffering patients. It may be caused by contractures [3],[5],[6] or muscle hypertonicity [7],[8],[9]. Figure 1.1 [10] shows the different types of cerebral palsy, which parts of the brain is affected by these different types and what are the consequences accordingly.

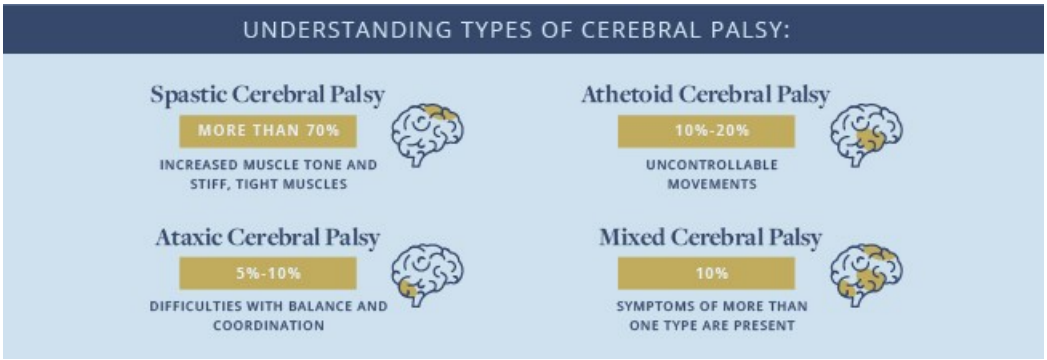

Figure 1.1 Different types of cerebral palsy [10].

1.2 Spastic Muscle Mechanics

The exact mechanism of muscle resistance against joint extension is not clear for the patients suffering from spastic cerebral palsy. Active and passive features of spastic skeletal muscles can be associated with this. There can yet be a limiting factor for joint range even if there is no active force exertion on the spastic muscle and the passive forces are expected to be high [5],[11],[12]. Unexpectedly, relatively lower muscle passive force can be seen during intraoperative measurements, for spastic flexor carpi ulnaris muscle, in the upper extremity [13],[14]. In the lower extremity on the other hand, there is no direct calculation and measurement as such and demonstration of higher passive muscle stiffness is considered as typical. This has been addressed by the procedures involving muscle biopsies [15], and dynamometry and ultrasound shear wave elastrography [16]. There are various studies both promoting and declining the effect of spasticity on the gait disorder in accordance with the active muscle stiffness [17],[18],[19],[20]. The limited joint motion of a cerebral palsy patient due to the pathological reasons is obvious through the active and passive muscle forces of a human being and their abilities to update joint moments can be computed as a function of join angle with the help of intra-operative tests [21]. It is shown that the gracilis (GRA) and semitendinosus (ST) muscles of a patient with cerebral palsy generate low forces when the knee positions are flexed [22],[23],[24]. However, there is no study presented yet to correlate the muscle forces with muscle-tendon complex lengths observed during the relevant gait cycles.

1.3 Aim of the Thesis

This study aims at determining muscle-tendon complex length changes during the gait cycle and finding a correlation between the single muscle active and passive forces with changing muscle-tendon complex lengths. For instance, maximum GRA muscle force was detected at 0 or 60 degrees of knee angles but no data directly as a function of muscle-tendon complex length has been achieved so far. This kind of

correlation was aimed to be obtained by finding equivalent muscle-tendon complex length and muscle force values measured by using different tools. For the same hip and knee angles, related force and length values were targeted to be correlated. In addition, no range could be achieved for the muscle-tendon complex length of spastic GRA and ST muscles.

Therefore, the aim of the study is to determine (1) if the range for spastic muscle-tendon complex length is comparable to that of healthy muscle and (2) how spastic muscle force changes as a function of muscle-tendon complex length.

2. METHODS

2.1 Intraoperative Testing Procedure

Surgical procedure was performed to measure the GRA and ST muscles active and passive forces, in Istanbul University Department of Medicine along with the agreement with the guidelines of Helsinki declaration. Experimental data was collected from seven different patients who all were informed before, and this operation was approved by a Committee on Ethics of Human Experimentation at Istanbul University, Istanbul. The work was legally approved by the patients and/or their parents with an official consent.

The surgical study contained seven patients. The oldest patient was 13 years old and the youngest one was 6 years old, and the group had the mean value of 9 years and 2 months with the standard deviation of 2 years 10 months. All the seven patients had cerebral palsy disease but none of them was subjected to prior remedial surgery before. Gross Motor Functional Classification System (GMFCS) level was II for all of these patients. Considering the Modified Tardieu Scale and Modified Ashworth Scale scores, popliteal angles were measured related to their clinical spasticity scores.

Before the surgery to be performed, gait analysis assisted the study in order to obtain an objective diagnostic assessment. This data was utilized to create a correlation between joint angle-muscle force measurements of the spastic muscle level and typical patient motion characteristics. All in all, requirement of the remedial surgery by releasing hamstrings and hip adductors was proven with the help of clinical examination performed before the operation which showed extremely limited knee range of motion.

Helen Hayes Marker Placement Protocol [25] was fulfilled in order to establish a motion analysis system (ELITE 2002, BTX Bioengineering, Milano, Italy) by using six

infrared cameras and two force plates (Kistler Instrumente AG, Winterthur, Switzerland). Bilateral markers were located at the metatarsal head V, heel, lateral malleolus, tibial wand, femoral lateral epicondyle, femoral wand, and anterior superior iliac spine (ASIS). One single marker was located on the sacrum and the other one was placed on the seventh cervical vertebrae (C7) so as to evaluate the shoulder tilt relative to the horizontal axis combined with the two different shoulder markers placed on the flat parts of the acromion. In addition, this marker enabled to detect the initiation of walking as well. Gait analysis results were used to detect the visible hip and knee angles during gait of the patients, and finally used to determine the joint positions will be used on intraoperative muscle mechanical testing.

Seven patients were operated on bilaterally and datasets were collected for ten different limbs. (For three of the patients, separate experiments were performed on both legs.) For the remainder patients, only one leg was experimented due to time limitations imposed by subsequent multilevel surgery. Thanks to the intraoperative measurements, passive state ST and GRA muscle forces were measured (condition I) and the active muscle forces were measured again after stimulation of GRA and ST muscles selectively (condition II). These measurements we performed at ten different joint positions containing 20 degrees and 45 degrees hip angles, along with the knee angles of $0^\circ - 30^\circ - 60^\circ - 90^\circ - 120^\circ$.

These specific hip and knee angles were chosen based on the gait analyses [26]. In the end, a total of ten sets of knee angle vs. ST force and knee angle vs. GRA force data were obtained.

2.2 Musculoskeletal Modeling

By aiming to detect the different muscle-tendon complex length values for specific hip and knee angles, experimental data was gathered from seven different patients in C3D (coordinate 3D) file format related to their static (standing) pose and walking cases on the force plates. Three different dynamic trials were analyzed for each patient.

In order to use this static and dynamic data as an input for OpenSim [27],[28] which is open source software in order to create models and form simulations for musculoskeletal structures in action, they need to be transformed into track row column (TRC) file format. Another open source software, Mokka [29] was applied to serve this purpose. With the help of Mokka, experimental data of the patients was converted to input files for the OpenSim model.

It is required to reach action dynamic simulation(s) if one would like to examine internal loads in the skeletal system or work on the neuromuscular stability. In parallel, this kind of simulations are also useful for the identification of sources that belong to the pathological movement, and develop better treatment schedule afterwards. OpenSim was developed as a freely available and open source model base which lets the users to obtain models and simulations accordingly. This system is applied in order to study dynamic of human beings with pathological gait and analyze the biomechanical effects of the treatment plan, by using a library of models and simulations created before.

For the seven patients one by one, personalized musculoskeletal models were developed by modifying the OpenSim Gait_2392 model. The Gait_2392 model contains 92 muscle-tendon actuating units so that 76 different muscles in the lower extremities and torso are represented with 23 degree of freedoms. The default and unscaled model stands for a human being patient with 180 centimeters length and 75160 grams weight. This already developed model can be found, used and modified in OpenSim for calculating forces and moments, the updates on the geometry of the muscle and skeletal systems after a surgical operation or physiotherapy, muscle derived walking or running computational analysis.

In order to receive the precise outcomes from the model analysis, generic model was required to be modified and this goal was reached with the scaling operation. Basically, scaling tool changes the dimensions and measurements of the Gait_2392 model, therefore it can represent a real particular patient as much as possible. Typically, scaling operation is processed with the comparison of experimental marker data placed on the actual patient and virtual markers located on the model, along with the length and

weight updates from model to the actual patient. TRC static files of the patients gathered from the gait analysis were used as the input files for scaling operation in which the experimental markers were checked against the virtual markers. The dimensions from the experimental markers were measured with motion capture equipment where the virtual markers are positioned in the anatomical relevance. The scale factors are computed by comparing the distances between experimental markers relatively to the virtual markers. This computation was applied by using the setup file that contains the reference for static experimental data in TRC format, length and weight of the patients, weights given to the markers having exactly the same name marker names in experimental data and gives out an output file to solve the inverse kinematics problems for the next steps.

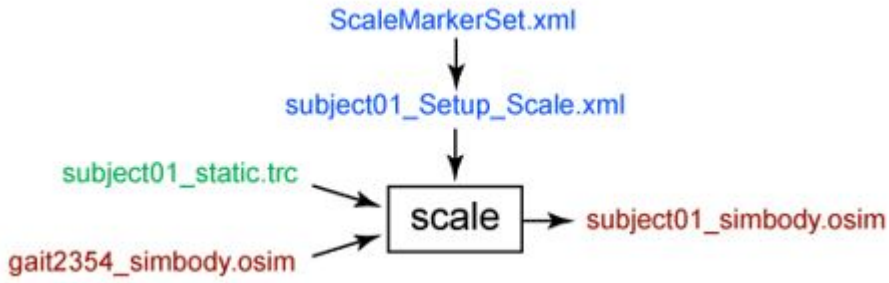

Figure 2.1 Input and output elements of scaling tool. Experimental data are shown in green; OpenSim files are in red; settings files are in blue.

Once the personalized model was created via scaling operation, the inverse kinematics tool was used to calculate muscle-tendon complex length, knee and hip angles correspondingly as it steps through each time frame of experimental data and arrange the positions of the model again in a pose that 'best matches' experimental marker and coordinate data for that time step. It is highly critical to reach proper and accurate data as an outcome from inverse kinematics operation so as to use it for force computation tools such as static optimization.

Setup files should be created for inverse kinematics operation with a similar procedure of scaling setup files. These setup files need to contain the same markers (with the same marker names and weights for calculation again) for the consistency and this time, they refer to the dynamic experimental data of the patients in TRC format.

For different cases, setup file uses the output from the scaling operation and different walking cases as input files for inverse kinematics within a specified time range. In this time range, this operation enables the users to observe the changing trends for muscle-tendon complex lengths, fiber lengths, joint angles (knee and hip angles for this case). Moreover, it starts the procedure for force analysis that can be processed after the static optimization tool which can analyze the active, passive, total fiber forces.

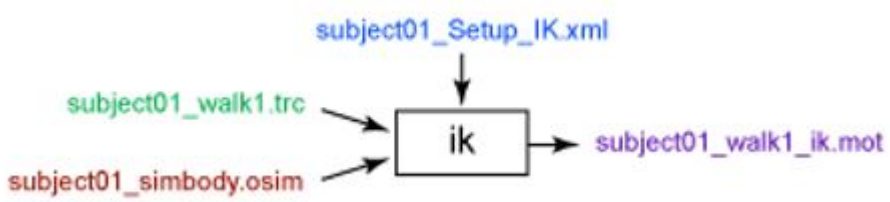

Figure 2.2 Input and output elements of inverse kinematics tool. Experimental data are shown in green; OpenSim files are in red; settings files are in blue.

It is possible to see the trend plots for knee angle, hip angle and muscle-tendon complex length after the inverse kinematics is run successfully. For the gracilis muscle, all these three features were calculated for the different walking experimental data of the patients.

During intraoperative measurements, active and passive forces of ST and GRA muscles were measured for some specific hip angle and knee angle couples. Using gait analysis data processed via OpenSim, it was possible to achieve the data for entire gait cycle, which contains intervals with the identified hip and knee angles. In order to obtain the relevant data, hip angle values of 20° and 45° were set as the absolute and exact conditions for the model gait analysis as well, where the knee angle equivalents were adjusted to 0°, 30° and 60° values with plus or minus 3° tolerances. Consequently, the computations were completed for the knee angle intervals between 0°-3°, 27°-33°, and 57°-63°; provided that the hip angles were precisely equal to 20° and 45°.

Considering that the exact values of 20° and 45° hip angle values cannot be seen on the dataset acquired from OpenSim, some extra calculations need to be processed. In order to achieve this goal, the time intervals in which the 20° or 45° values are

involved were designated and knee angle values along with the muscle-tendon lengths equivalent to these specific values are calculated. This procedure was followed for 10 limbs that belong to the 7 different patients so that the muscle-tendon complex lengths for gracilis and semitendinosus muscles are obtained for the conditions the intraoperative measurements are performed. Consequently, muscle-tendon complex lengths and equivalent muscle active and passive forces are gained for some specific hip angle-knee angle couples.

3. RESULTS

3.1 Muscle-Tendon Complex Length Changes

Figure 3.1 shows spastic ST and GRA muscle-tendon complex length changes as a function of percent gait cycle.

For the ST, healthy muscle-tendon complex length changed by 13% between its minimum and maximum values. Patient specific models indicate that the patientsâ muscle-tendon complex lengths change by 9.9% +/- 2.2% (mean +/- standard deviation). The maximum change was observed by 14% for Limb 6 and the minimum change was observed by 7% for Limb 7, between the minimum and maximum length values in the curves of the patients.

For the GRA, healthy muscle-tendon complex length changed by 8% between its minimum and maximum values. Patient specific models imply that the patientsâ muscle-tendon complex lengths change by 6.8% +/- 1.7% (mean +/- standard deviation). The maximum change was observed by 9% for Limb 6 and the minimum change was observed by 4% for Limb 4, between the minimum and maximum length values in the curves of the patients.

These results suggest that the spastic muscles studied show similar characteristics to the typically developed (TD) healthy muscle (the black threadline).

3.2 Spastic Muscle Force Changes as a Function of MTL

Patient specific models were developed in order to obtain different muscle force trend curves against the increasing muscle-tendon complex lengths. The figures in the following sections suggest that the muscle forces have a tendency to increase with the

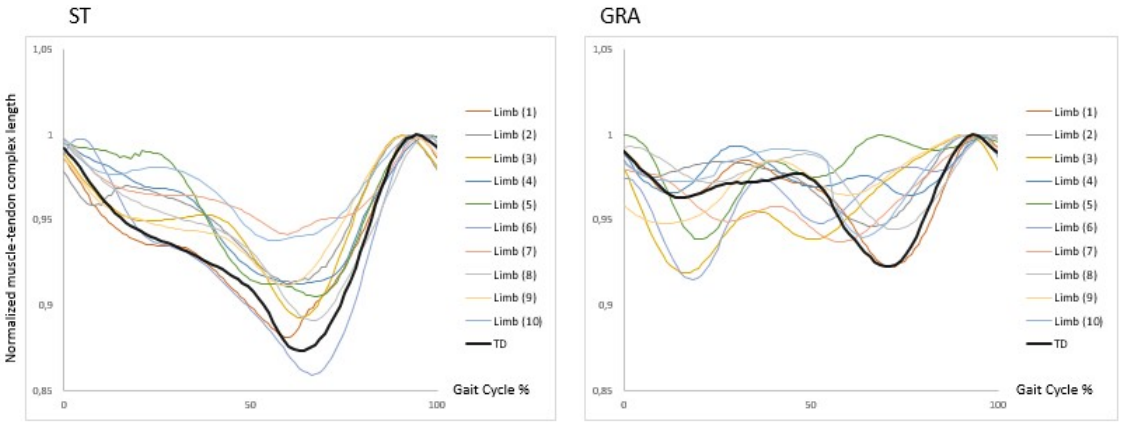

Figure 3.1 Normalized muscle tendon unit length graph against gait cycle percentage for the GRA and ST muscles of ten different limbs.

increasing muscle tendon complex lengths. In addition, the dominant component of the total force is the active muscle force. For GRA, the maximum active muscle force is 5.62 times higher than maximum passive force in average. For ST, the maximum active muscle force is 3.82 times higher than maximum passive force in average.

3.2.1 Patient 1 - Limb 1

Figure 3.2 shows the change of GRA and ST muscle-tendon complex lengths during the gait cycle. It could be seen that both two muscles were persistent on their actions between the gait relevant time zones of around 0.67 seconds and around 3.90 seconds.

Figure 3.2 Limb 1 GRA and ST muscle-tendon complex length changes during the gait cycle.

Table 3.1 shows that eight different data points for GRA and eight for ST muscles, that the muscle length and muscle force could be associated. No muscle force measurement was possible for the 120° knee angle, because there was no space to bend the leg related to the patients position on the stretcher. This consequently resulted in 8 data points instead of 10. Three of those were observed during the actual gait cycle of the patient as recorded during his/her gait. These points are highlighted in the table.

Figure 3.3 for the GRA muscle was obtained by using the dataset in Table 3.1. This figure shows that muscle passive force increased consistently while the muscle-tendon complex length increases in parallel. Therefore, the maximum passive force was observed with the maximum muscle-tendon complex length. The active force increased as well until its maximum value and slightly decreased afterwards. In summary, muscle

Table 3.1
Muscle-tendon complex length and muscle force data of Limb 1 for different hip and knee angles.

		GRA			ST		
HA	KA	Cond I (N)	Cond II (N)	MTL (m)	Cond I (N)	Cond II (N)	MTL (m)
45	120	-	-	0.384	-	-	0.424
45	90	0.299	66.550	0.398	1.969	78.940	0.435
45	60	1.449	73.680	0.415	7.706	76.610	0.455
45	30	8.859	72.860	0.433	28.266	77.380	0.478
45	0	22.759	73.770	0.446	44.396	87.630	0.498
20	120	-	-	0.373	-	-	0.398
20	90	0.905	62.010	0.387	0.465	36.450	0.408
20	60	0.005	72.470	0.404	0.93	57.690	0.428
20	30	3.325	79.200	0.421	4.852	53.310	0.451
20	0	19.455	74.220	0.434	29.262	88.440	0.471

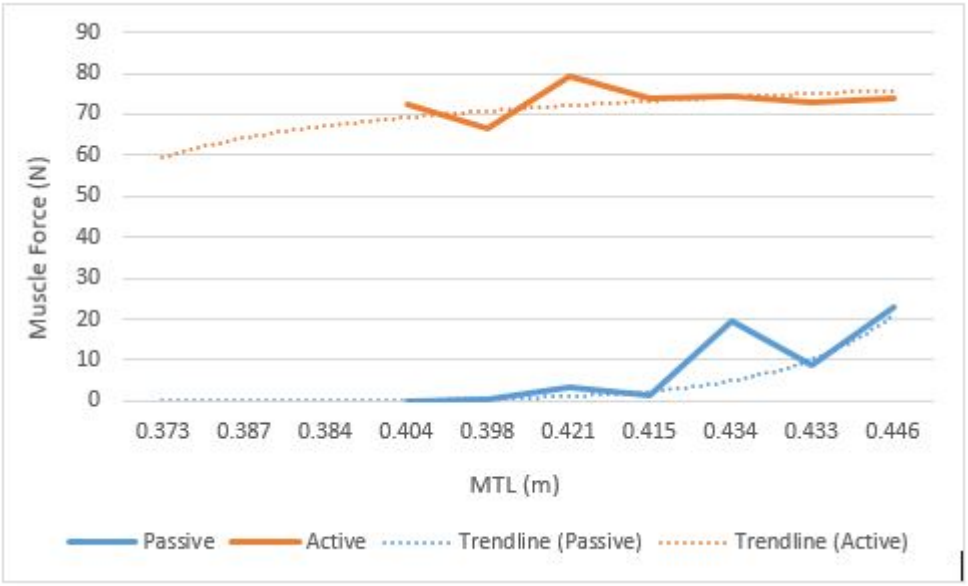

Figure 3.3 Limb 1 GRA muscle-tendon complex length vs. muscle passive and active forces.

forces tended to increase with the increasing muscle-tendon complex length, based on the trend lines and the value changes between minimum and maximum muscle-tendon complex lengths.

According to the Figure 3.4, passive force of ST muscle increased consistently similar to that of the GRA of the same patient. The maximum force value was encountered at the maximum muscle-tendon complex length. For the active force on the other hand, there was no consistent behavior as there were several increasing and decreasing

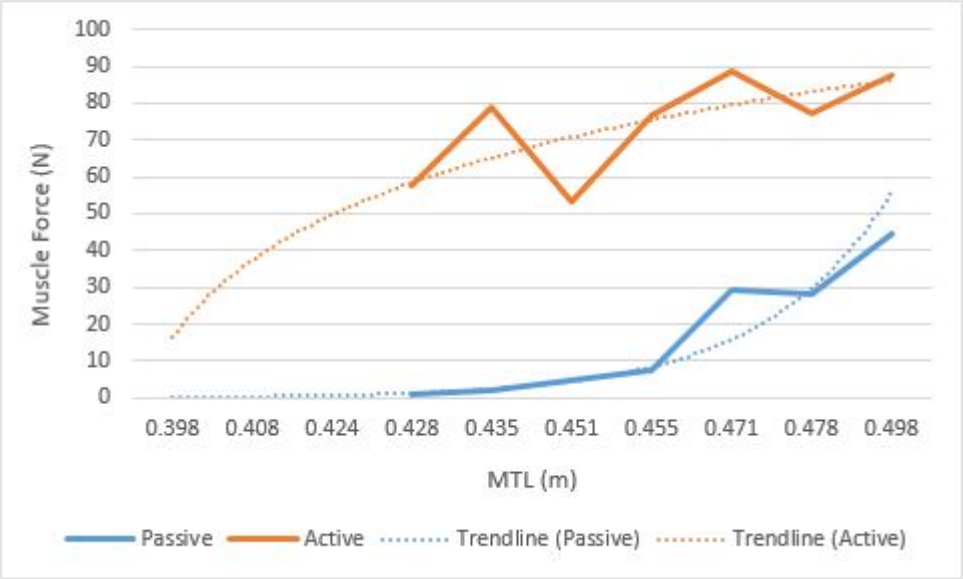

Figure 3.4 Limb 1 ST muscle-tendon complex length vs. muscle passive and active forces.

force trends. However, relatively higher force values corresponded with the relatively higher muscle-tendon complex lengths in the second half of the graph.

3.2.2 Patient 1 - Limb 2

Figure 3.5 shows that, the muscle-tendon complex length trend is consistent starting from the beginning of the action and until around 3.29 seconds. Similar to the Limb 1, the other limb of the same patient, three persistent curves could be observed for both GRA and ST muscles and the maximum ST muscle-tendon complex length value was higher than the maximum GRA muscle value.

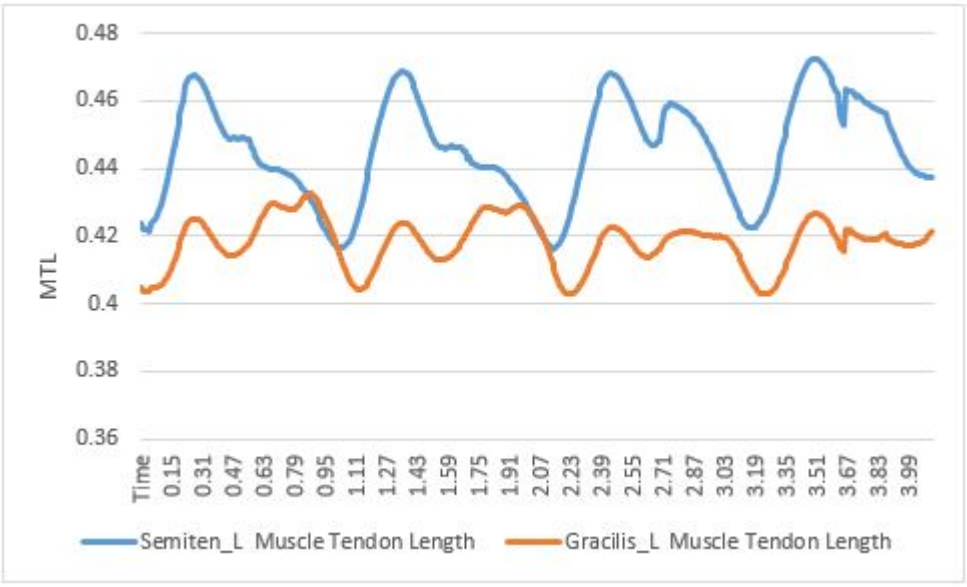

Figure 3.5 Limb 2 GRA and ST muscle-tendon complex length changes during the gait cycle.

Table 3.2 shows the muscle force and muscle-tendon complex length values of the second limb of Patient 1. Similar to the Limb 1, only 8 different data points were obtained because of the patent position on the stretcher. As it can be seen, OpenSim gives out exactly the same muscle-tendon complex length values for Limb 2, which is the left leg of Patient 1, as Limb 1, which is the right leg of Patient 1. It can be concluded that OpenSim results same values for the different limbs of a patient. (This phenomenon will be verified for the following patients which will be measured for two different limbs.) 20° hip angle with 0° and 30° knee angles could be seen during the real gait cycle of the patient this time ad these two rows are painted in the Table 3.2.

According to the Figure 3.6, it can be said that GRA passive muscle force does not change significantly with the increasing muscle-tendon complex length. In total, it

Table 3.2
Muscle-tendon complex length and muscle force data of Limb 2 for different hip and knee angles.

		GRA			ST		
HA	KA	Cond I (N)	Cond II (N)	MTL (m)	Cond I (N)	Cond II (N)	MTL (m)
45	120			0.384			0.424
45	90	28.431	46.96	0.398	5.572	44.22	0.435
45	60	29.049	81.74	0.415	6.552	76.88	0.455
45	30	34.969	168.66	0.433	10.002	89.79	0.478
45	0	55.059	184.4	0.446	37.002	60.75	0.498
20	120			0.373			0.398
20	90	33.394	99.79	0.387	1.575	18.24	0.408
20	60	36.419	132.15	0.404	1.779	70.25	0.428
20	30	41.959	41.959	0.421	2.825	72.74	0.451
20	0	62.159	128.63	0.434	11.175	65.93	0.471

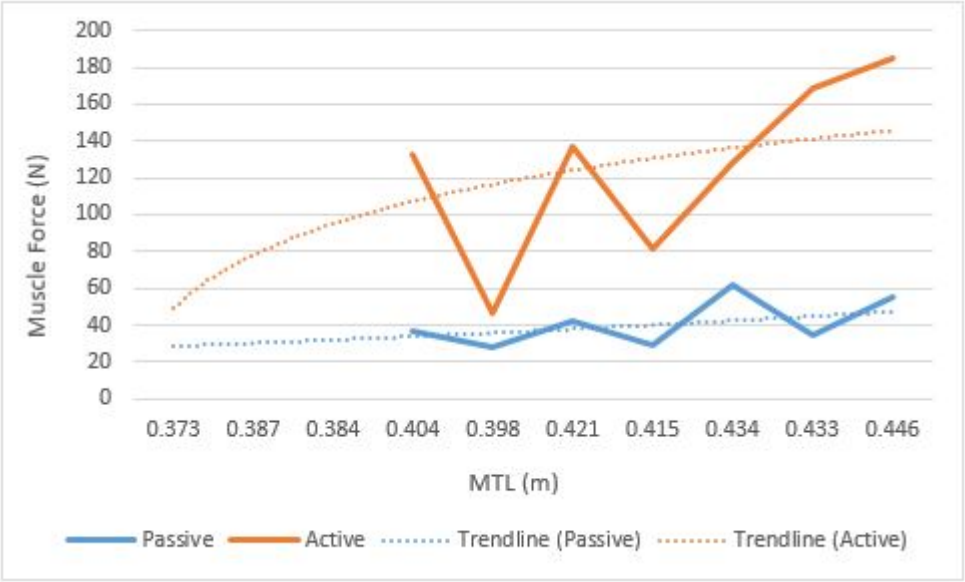

Figure 3.6 Limb 2 GRA muscle-tendon complex length vs. muscle passive and active forces.

can be said that the passive force was slightly increased compared to the minimum and maximum muscle-tendon complex length values. The GRA active force on the other hand was highly inconsistent and no correlation could be achieved between the muscle-tendon complex length and active muscle force. Although there is an increase on the muscle force values measured with minimum and maximum muscle-tendon complex lengths, the actions in the interspace was without any pattern. Another surprising finding was the active and passive force values were very close to each other for some

specific data points.

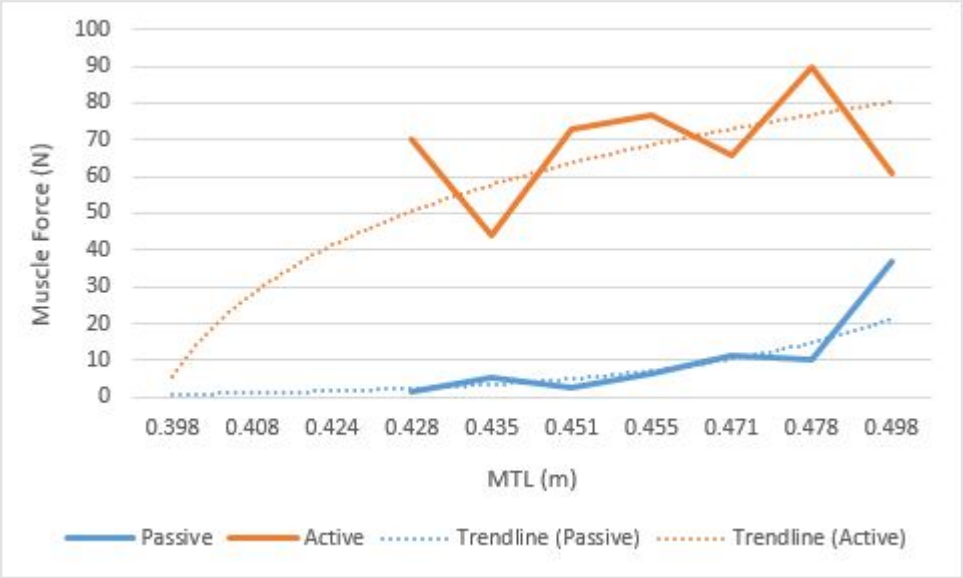

Figure 3.7 Limb 2 ST muscle-tendon complex length vs. muscle passive and active forces.

Similar to the GRA, ST passive muscle force was quite steady for the changing muscle-tendon complex length, except for the final jump. In total, it can be said that there is a tendency to increase related to the passive muscle force. Active muscle force though does not have any pattern again similar to the GRA muscle, as the graph contains several increasing and decreasing force trends and there is no direct correlation between the muscle-tendon complex length and active muscle force.

3.2.3 Patient 2 - Limb 3

There were persistent muscle-tendon complex length behaviors for both ST and GRA muscles. It can be seen between the around 2.04 seconds and around 3.84 seconds in the Figure 3.8. The maximum values for ST and GRA muscles were at the similar levels dissimilar to the other limbs. Two repeating trends could be observed during the gait cycle for both GRA and ST.

Figure 3.8 Limb 3 GRA and ST muscle-tendon complex length changes during the gait cycle.

Table 3.3 shows the muscle-tendon complex length and muscle force values for the GRA and ST muscles of Limb 3. There were 10 data points that had both force and length values, in order to create the graphs. One single condition with 20° hip angle and 30° knee angle was observed during the actual gait cycle.

When the GRA muscle force values were checked for different muscle lengths from the Figure 3.9, it can be said that the maximum passive force value was aligned with the maximum muscle-tendon complex length one more time. Active muscle force had a tendency to increase with the increasing muscle-tendon complex length in general, although it showed a separate characteristics and the maximum value was designated before the maximum length value.

Table 3.3
Muscle-tendon complex length and muscle force data of Limb 3 for different hip and knee angles.

		GRA			ST		
HA	KA	Cond I (N)	Cond II (N)	MTL (m)	Cond I (N)	Cond II (N)	MTL (m)
45	120	1.402	18.080	0.309	0.31	0.11	0.344
45	90	4.095	36.530	0.32	0.38	8.200	0.353
45	60	4.120	51.320	0.334	2.980	18.770	0.37
45	30	9.775	47.220	0.349	9.560	54.100	0.388
45	0	29.362	42.810	0.36	24.540	12.530	0.405
20	120	0	9.050	0.299	0.366	0.26	0.321
20	90	1.056	39.800	0.31	0.526	19.840	0.329
20	60	1.654	51.300	0.325	1.186	36.880	0.346
20	30	7.546	44.400	0.339	2.976	16.710	0.365
20	0	24.480	45.090	0.35	16.286	8.270	0.382

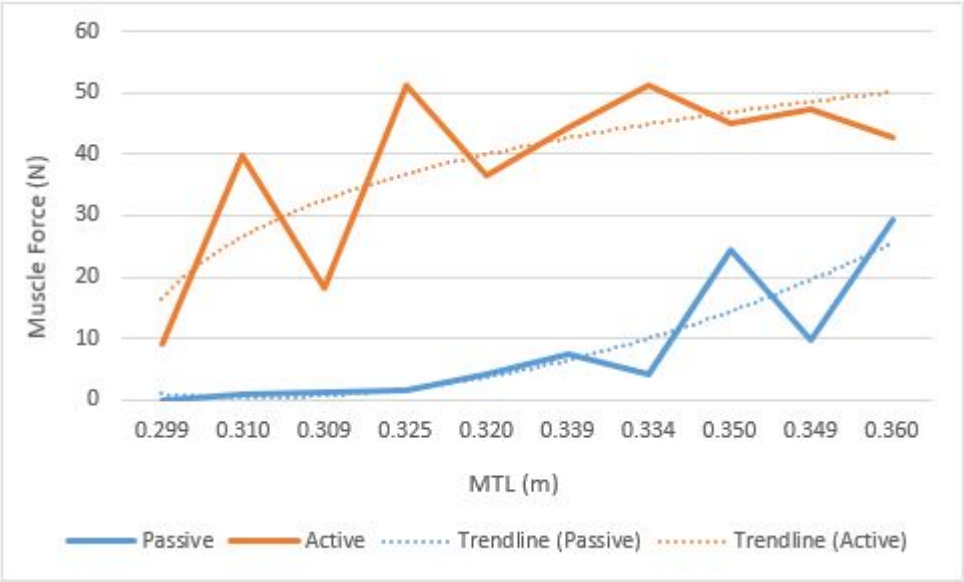

Figure 3.9 Limb 3 GRA muscle-tendon complex length vs. muscle passive and active forces.

ST passive force from the Figure 3.10 was observed at the maximum muscle-tendon complex length value as consistent with the previous muscle force characteristics. There is no direct trend could be observed for the behavior of active muscle force on the other side, because of the huge slope values between successive muscle-tendon complex lengths. Nonetheless, it could be seen that maximum force value was observed at the second highest muscle-tendon complex length point.

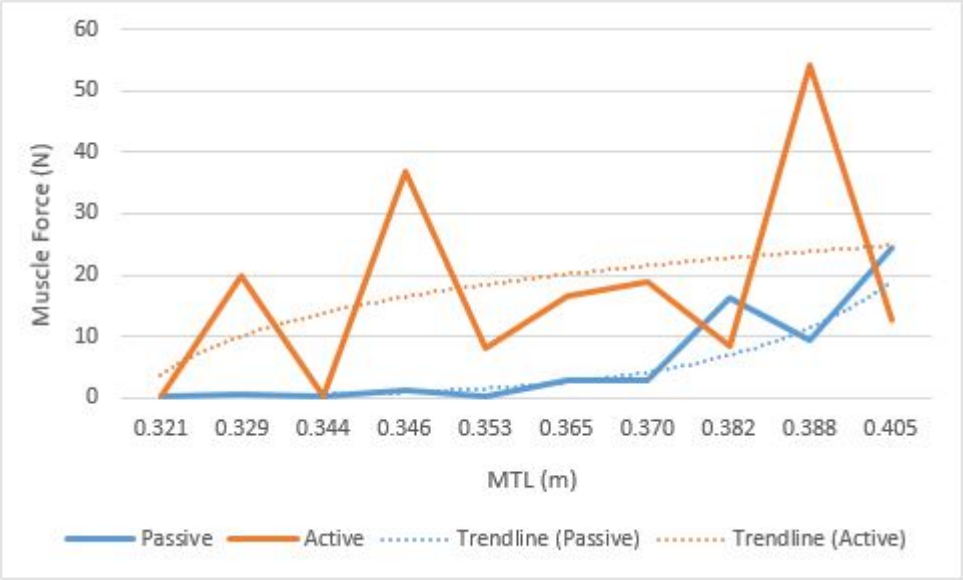

Figure 3.10 Limb 3 ST muscle-tendon complex length vs. muscle passive and active forces.

3.2.4 Patient 3 - Limb 4

The trend for Limb 4 shows that there is a repeating pattern between the 4.04 seconds and 7.03 seconds as it can be seen on the Figure 3.11. Three repeating similar cycles could be observed for ST and fading pattern for GRA could be seen as well.

Figure 3.11 Limb 4 GRA and ST muscle-tendon complex length changes during the gait cycle.

Ten different data points could be collected for muscle active and passive forces during the intraoperative measurements and the equivalent muscle-tendon complex length values could be calculated for both GRA and ST. For this limb of Patient 3, the 30° knee angle could be observed during the real gait cycle along with the both 20° and 45° hip angle values.

Table 3.4
Muscle-tendon complex length and muscle force data of Limb 4 for different hip and knee angles.

		GRA			ST		
HA	KA	Cond I (N)	Cond II (N)	MTL (m)	Cond I (N)	Cond II (N)	MTL (m)
45	120	0.759	11.440	0.247	0.83	3.610	0.281
45	90	0.759	34.800	0.259	0.13	7.970	0.291
45	60	0.849	54.610	0.275	1.884	12.980	0.309
45	30	1.529	48.910	0.291	4.270	14.490	0.328
45	0	5.409	32.100	0.302	5.470	17.510	0.346
20	120	1.133	22.000	0.238	0	1.300	0.258
20	90	1.215	32.100	0.25	1.070	7.110	0.268
20	60	1.430	45.740	0.266	1.840	5.860	0.286
20	30	2.545	44.670	0.281	2.460	12.070	0.306
20	0	5.323	44.880	0.292	3.470	26.030	0.323

The GRA muscle passive force values can be said to be highly stable with a slight increase against the increasing muscle-tendon complex length. This kind of a behavior is consistent with the passive force trends of other limbs analyzed so far. For the active GRA muscle force, there is no direct correlation between the muscle force and muscle-tendon complex length as increasing and decreasing force trends can be seen on the Figure 3.12. In total, it can be asserted that there is a tendency to increase comparing the active force values recorded for minimum and maximum muscle-tendon complex lengths.

The ST muscle passive force is also steady against the muscle-tendon complex length similar to the GRA muscle. As it can be seen on the Figure 3.13, it also ends with a slight increase consistently to the other passive force graphs. For the active muscle force, a tendency of force increase against the increasing muscle-tendon complex length can be mentioned despite couple of jumps could be observed. Nevertheless, direct correlation could be considered based on the total graph.

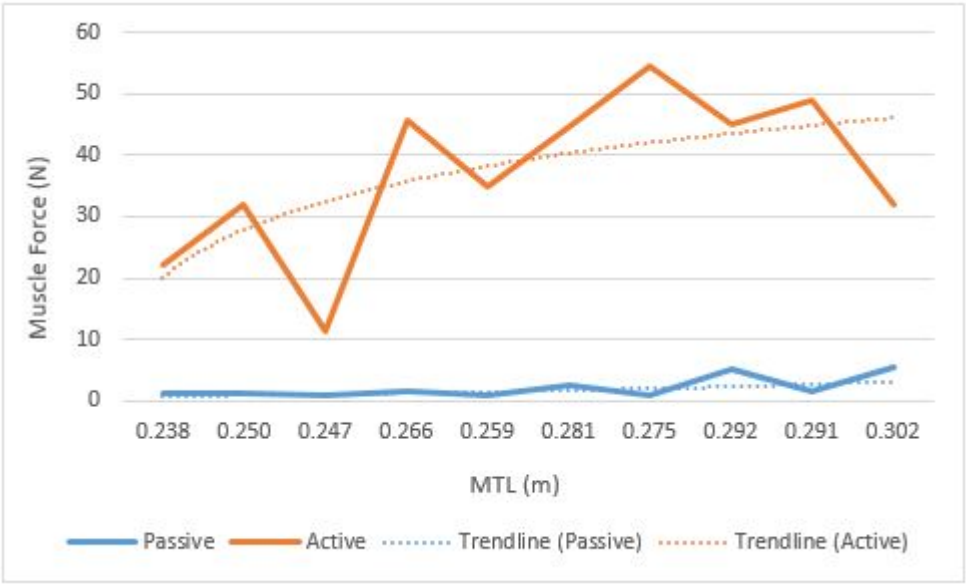

Figure 3.12 Limb 4 GRA muscle-tendon complex length vs. muscle passive and active forces.

Figure 3.13 Limb 4 ST muscle-tendon complex length vs. muscle passive and active forces.

3.2.5 Patient 3 - Limb 5

Two similarly repeating graphs could be detected on the Figure 3.14 for ST muscle of the Limb 5 between the 2.77 seconds and 6.27 seconds. For GRA muscle, three persistent patterns could be seen on the very same graph. Much the same with the other limbs, ST maximum muscle-tendon complex length value is higher compared

to the GRA maximum muscle-tendon complex length value.

Figure 3.14 Limb 5 GRA and ST muscle-tendon complex length changes during the gait cycle.

As planned for the entire study, ten different data points could be collected for active and passive muscle force values of GRA and ST muscles. The equivalent muscle-tendon complex lengths were recorded via OpenSim and as it can be seen on the Table 3.4 and Table 3.5, OpenSim simulations gave out exactly the same muscle-tendon complex length values for the two different limbs (Limb 4 and Limb 5) of the same patient (Patient 3), just like the Limb 1 and Limb 2 of Patient 1. For this specific Limb 5, 20° hip angle along with the 0° and 30° knee angle values could be observed during the actual gait cycle analysis.

The GRA muscle passive force does not change significantly with the increasing muscle-tendon complex length as it can be seen on the Figure 3.15, consistently to the other passive force patterns. Although there were some jumps for the active muscle force trend, a tendency for the force increase against the increasing muscle-tendon complex length could be spoken.

The passive muscle force of ST muscle is steady against the increasing muscle-tendon complex length similar to the GRA passive force. As expected, its graph ends with a slight increase. The active muscle force was steady as well, except the final

Table 3.5
Muscle-tendon complex length and muscle force data of Limb 5 for different hip and knee angles.

		GRA			ST		
HA	KA	Cond I (N)	Cond II (N)	MTL (m)	Cond I (N)	Cond II (N)	MTL (m)
45	120	0.962	16.290	0.247	0	5.890	0.281
45	90	1.018	20.700	0.259	0.24	10.960	0.291
45	60	1.624	44.150	0.275	1.210	10.070	0.309
45	30	3.492	51.050	0.291	5.800	14.280	0.328
45	0	7.058	29.860	0.302	19.010	71.890	0.346
20	120	1.229	7.170	0.238	0.257	6.580	0.258
20	90	1.399	24.000	0.25	0.297		0.268
20	60	1.809	52.050	0.266	0.027	12.280	0.286
20	30	4.849	53.060	0.281	0.397	12.800	0.306
20	0	13.519	30.240	0.292	3.367	20.260	0.323

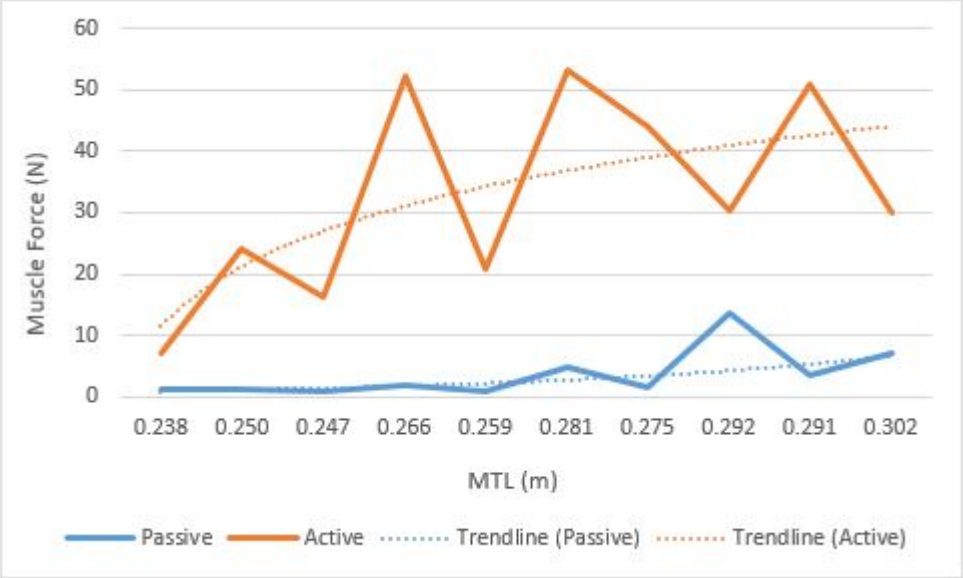

Figure 3.15 Limb 5 GRA muscle-tendon complex length vs. muscle passive and active forces.

jump in the end of the graph. All in all, active muscle force can be said to be increased with the increasing muscle-tendon complex length when the force values are compared for minimum and maximum muscle-tendon complex length values.

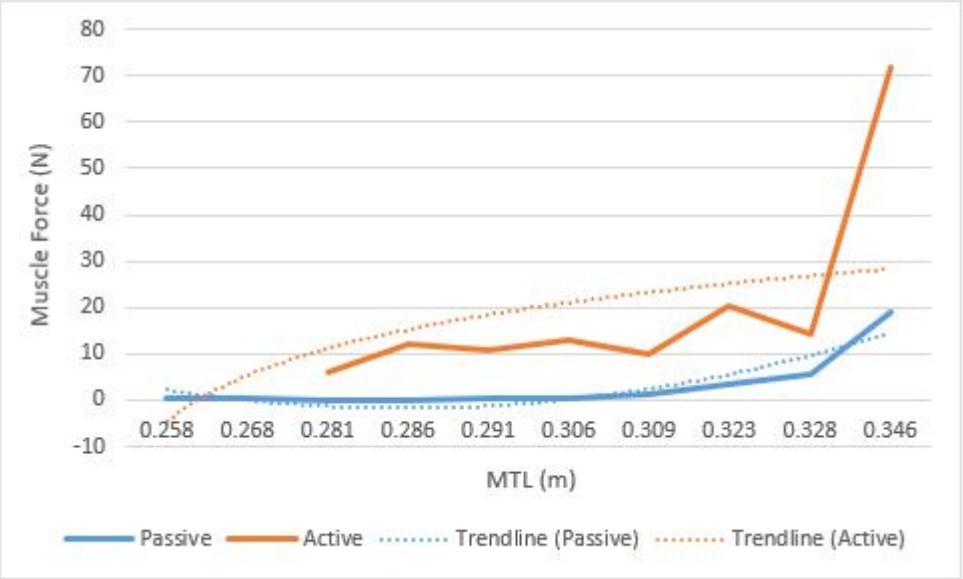

Figure 3.16 Limb 5 ST muscle-tendon complex length vs. muscle passive and active forces.

3.2.6 Patient 4 - Limb 6

According to the Figure 3.17, four times repeating muscle-tendon complex length fluctuations could be observed for both ST and GRA muscles. These repeating cycles are placed between the 0.29 seconds and 3.50 seconds. Similar to the other patients and limbs, ST muscle maximum tendon length values are relatively higher compared to the GRA muscle values.

Table 3.6 shows the ten different data points containing the muscle-tendon complex length and active and passive force values. Among these ten different points, three of them were recorded during the real gait cycle of the Patient 4 which are 0°- 30°- 60° knee angle values with the 20° hip angle value for all. The maximum active force values were recorded with these three specific points for both GRA and ST muscles.

The passive force of Limb 6 GRA muscle can be accepted to be stable as it does not change substantially with the increasing muscle length. With the consistence of other muscle passive forces, the graph is completed with slight increase in the muscle force. The active force on the other hand tends to increase against the increasing

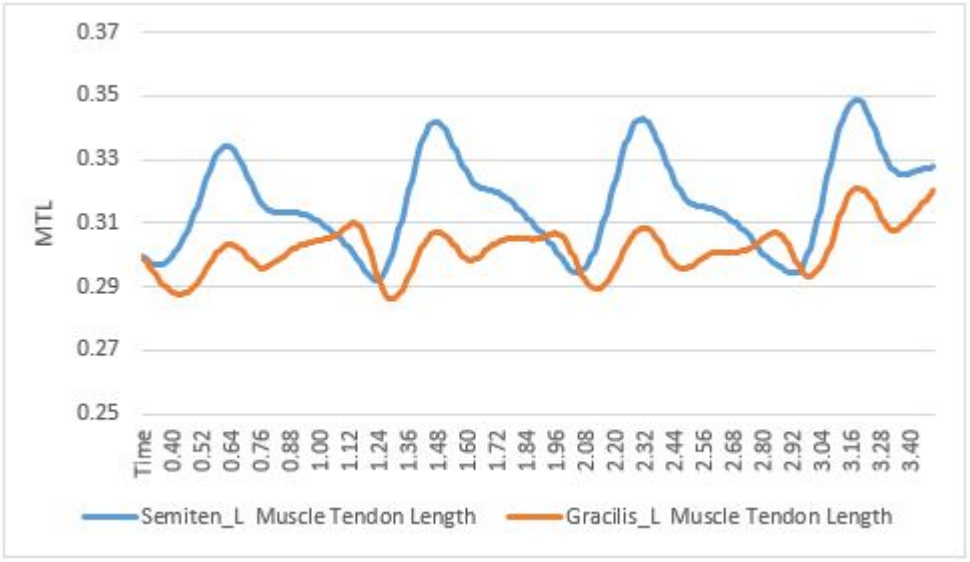

Figure 3.17 Limb 6 GRA and ST muscle-tendon complex length changes during the gait cycle.

Table 3.6
Muscle-tendon complex length and muscle force data of Limb 6 for different hip and knee angles.

		GRA			ST		
HA	KA	Cond I (N)	Cond II (N)	MTL (m)	Cond I (N)	Cond II (N)	MTL (m)
45	120	0.099	12.298	0.277	0.18	5.828	0.312
45	90	0.136	40.229	0.285	0.507	15.399	0.318
45	60	0.3	68.435	0.297	0.833	35.412	0.332
45	30	1.106	79.250	0.309	2.252	27.450	0.347
45	0	6.205	94.627	0.319	14.372	16.633	0.361
20	120	0.062	31.977	0.267	2.766	8.710	0.288
20	90	0.146	48.480	0.275	2.580	13.913	0.295
20	60	0.394	105.670	0.288	3.354	31.612	0.308
20	30	1.248	96.955	0.299	5.739	40.932	0.324
20	0	5.547	90.708	0.308	10.387	3.247	0.338

muscle length even with some decrements in the middle.

The passive force graph of ST muscle was similar to the GRA muscle and the other muscles passive force graphs. As it can be seen on the Figure 3.19, it stays almost steady and finishes the cycle with slight increase when the minimum and maximum values are compared. Dissimilarly, the active force of ST muscle behaved incoherently against the muscle-tendon complex length as there can be seen several increasing and decreasing force trends. The active muscle force values are close to each other for the

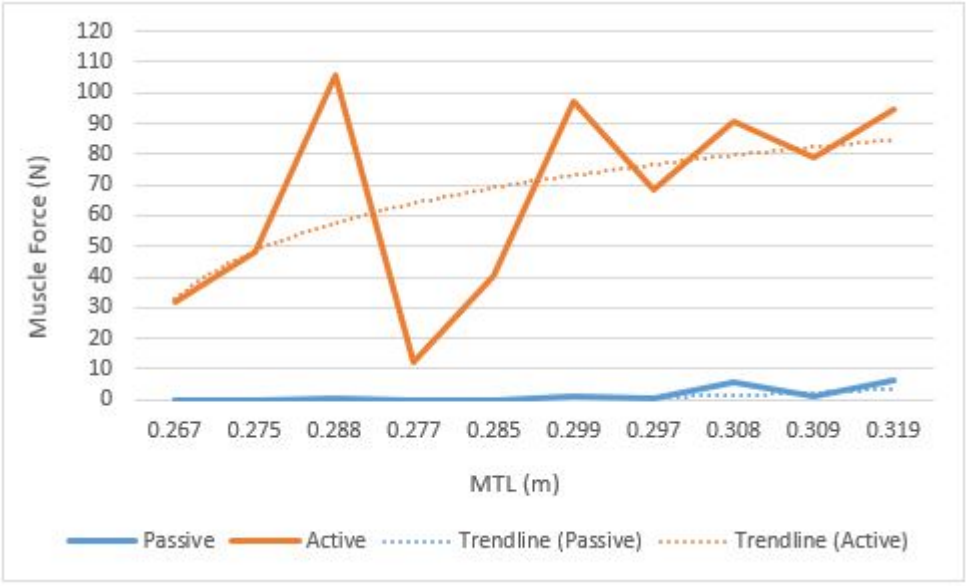

Figure 3.18 Limb 6 GRA muscle-tendon complex length vs. muscle passive and active forces.

minimum and maximum muscle-tendon complex length values.

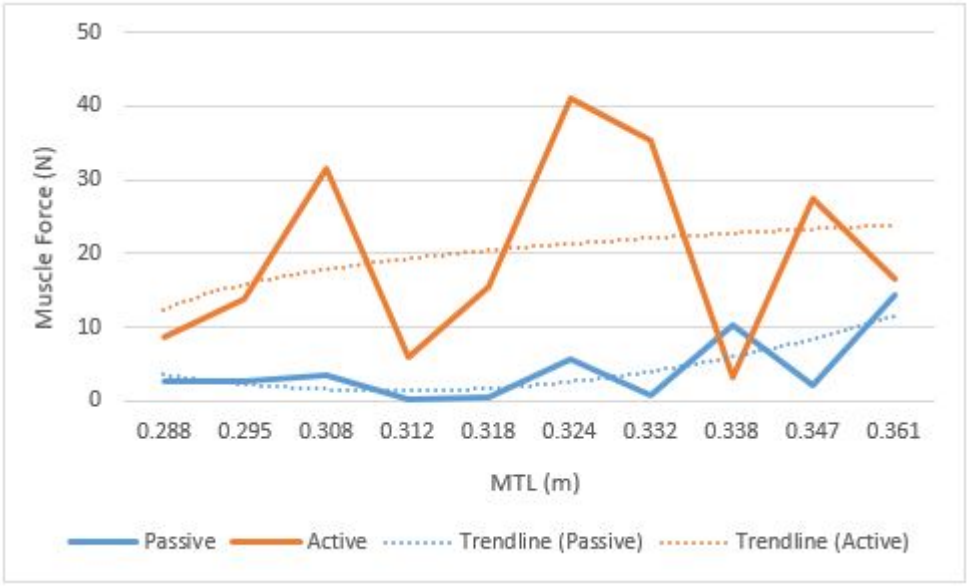

Figure 3.19 Limb 6 ST muscle-tendon complex length vs. muscle passive and active forces.

3.2.7 Patient 5 - Limb 7

As it can be seen on the Figure 3.20, the nearly repeating cycles of muscle-tendon complex lengths could be observed between the beginning of the gait cycle and 2.84 seconds for both GRA and ST muscles. Similar to the other limbs, ST muscle maximum tendon length values are higher compared to the GRA muscle maximum values.

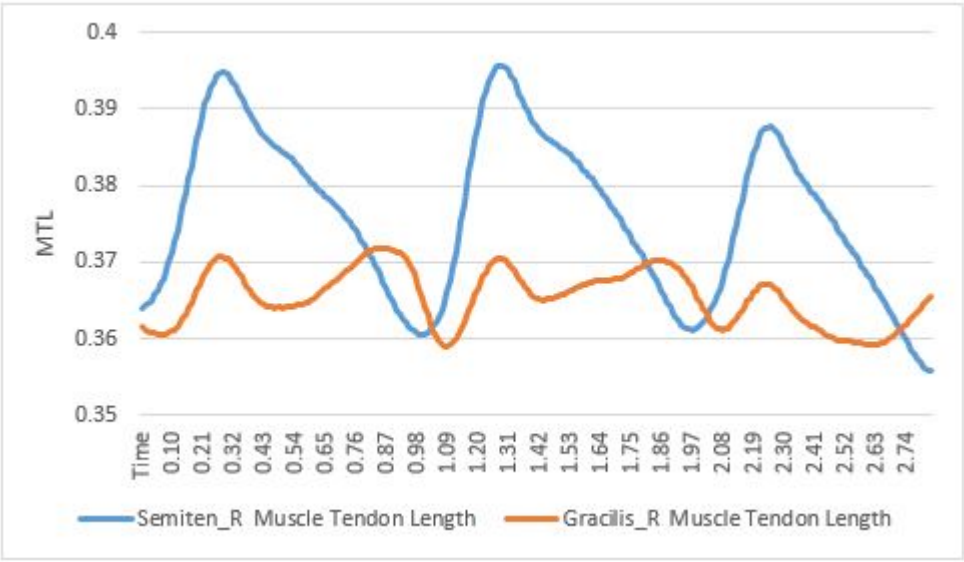

Figure 3.20 Limb 7 GRA and ST muscle-tendon complex length changes during the gait cycle.

The data points for Limb 7 of Patient 5 could be seen on the Table 3.7. One single point amongst them could be observed during the actual cycle which contains 20° hip angle and 30° knee angle values.

The passive force of Limb 7 GRA muscle can be said to be steady despite the insignificant increasing and decreasing force trends with low slopes. In total, it does not change considerably with the increasing muscle-tendon complex length and the initial and final force values are very close to each other equivalent to the minimum and maximum muscle-tendon complex length values. The active muscle force has a tendency to increase considering the comparison of starting and ending force values on the graph coinciding with the minimum and maximum muscle-tendon complex length values.

Table 3.7
Muscle-tendon complex length and muscle force data of Limb 7 for different hip and knee angles.

		GRA			ST		
HA	KA	Cond I (N)	Cond II (N)	MTL (m)	Cond I (N)	Cond II (N)	MTL (m)
45	120	9.926	54.806	0.326	7.196	3.925	0.368
45	90	15.968	36.891	0.338	7.202	67.430	0.377
45	60	17.155	56.520	0.353	7.233	63.080	0.394
45	30	16.541	54.540	0.369	7.331	79.709	0.414
45	0	8.196	38.970	0.381	7.797	43.570	0.432
20	120	13.290	22.089	0.315	7.197		0.34
20	90	6.281	49.380	0.326	7.196	46.298	0.349
20	60	7.694	55.404	0.342	7.203	63.786	0.366
20	30	17.486	69.362	0.357	7.252	79.243	0.386
20	0	10.086	80.390	0.368	7.434	51.467	0.404

Figure 3.21 Limb 7 GRA muscle-tendon complex length vs. muscle passive and active forces.

The ST muscle passive force does not change at all in the entire graph and it keeps almost the same value. This kind of behavior is consistent with the other passive force graphs. There is no direct correlation between the muscle-tendon complex length and active muscle force though as the graph on the Figure 3.22 contains several increasing and decreasing force trends.

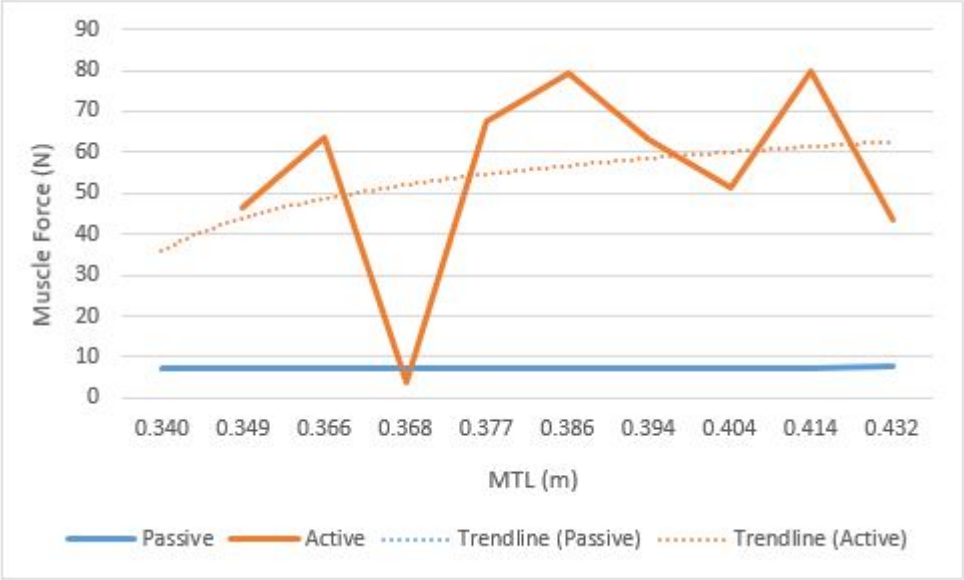

Figure 3.22 Limb 7 ST muscle-tendon complex length vs. muscle passive and active forces.

3.2.8 Patient 6 - Limb 8

Muscle-tendon complex length repeating cycles could be seen on the Figure 3.23 for the Limb 8 of Patient 6. The gait relevant cycle starts at 0.6 seconds and gets repeated for four times until 4.35 seconds for both GRA and ST muscles. Similar to the other limbs, maximum ST muscle tendon length observed is higher compared to the maximum GRA muscle-tendon complex length.

Table 3.8 contains the ten different data points collected during the intraoperative measurements and OpenSim simulations. Two of these ten data points could be seen during the real gait analysis of the patient in which the hip angle was equal to 20° and knee angle values were equal to 60° and 30°.

The passive muscle force of GRA does not change significantly with the increasing muscle-tendon complex length as expected. The active force of the same muscle has a tendency to increase with the increasing muscle-tendon complex length, when the total graph is analyzed although it contains two downhills as well. However, the total context points out that the GRA muscle of this limb contains a correlation between

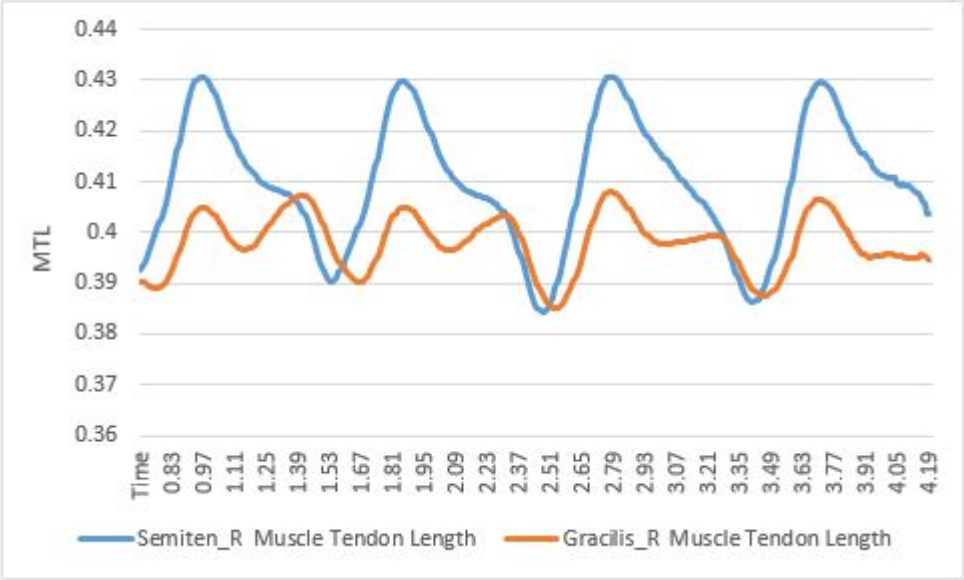

Figure 3.23 Limb 8 GRA and ST muscle-tendon complex length changes during the gait cycle.

Table 3.8
Muscle-tendon complex length and muscle force data of Limb 8 for different hip and knee angles.

		GRA			ST		
HA	KA	Cond I (N)	Cond II (N)	MTL (m)	Cond I (N)	Cond II (N)	MTL (m)
45	120	8.949	55.990	0.361	7.508	8.140	0.401
45	90	8.679	37.420	0.372	7.511	11.630	0.41
45	60	9.259	60.030	0.387	7.501	15.780	0.427
45	30	10.429	66.870	0.402	7.461	16.390	0.446
45	0	13.669	70.160	0.414	7.649	15.180	0.464
20	120	8.579	33.000	0.349	7.504	8.620	0.374
20	90	8.319	49.760	0.36	7.443	12.160	0.383
20	60	8.469	69.460	0.376	7.451	14.750	0.4
20	30	9.199	68.640	0.39	7.432	15.830	0.419
20	0	13.469	72.670	0.402	7.433	26.040	0.437

the muscle-tendon complex length and active muscle force.

Similar to the GRA muscle, ST muscle passive force does not change at all against the change of muscle-tendon complex length. Its straight line could be seen on the Figure 3.25. For the active muscle force, tendency for the increase can be still mentioned although it is not as apparent as GRA muscle.

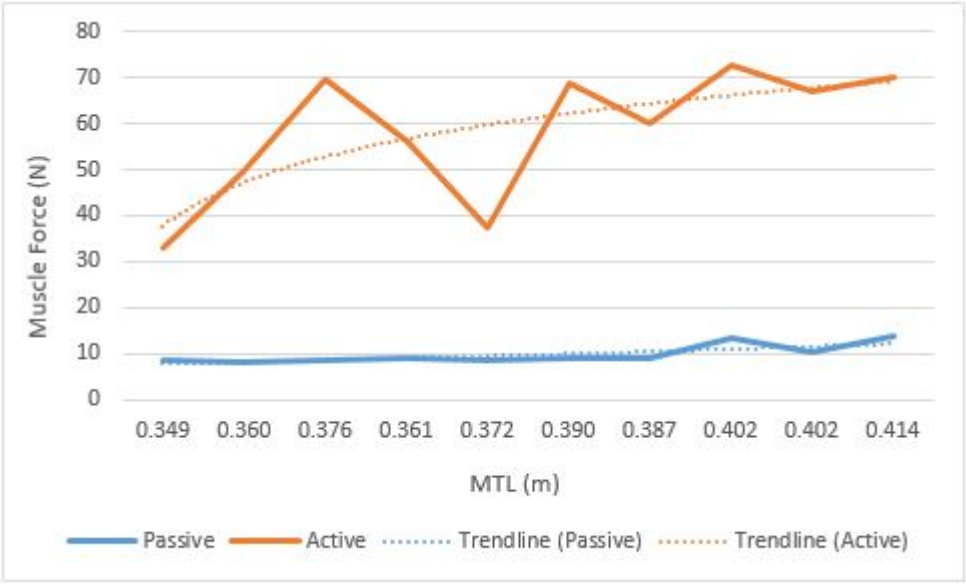

Figure 3.24 Limb 8 GRA muscle-tendon complex length vs. muscle passive and active forces.

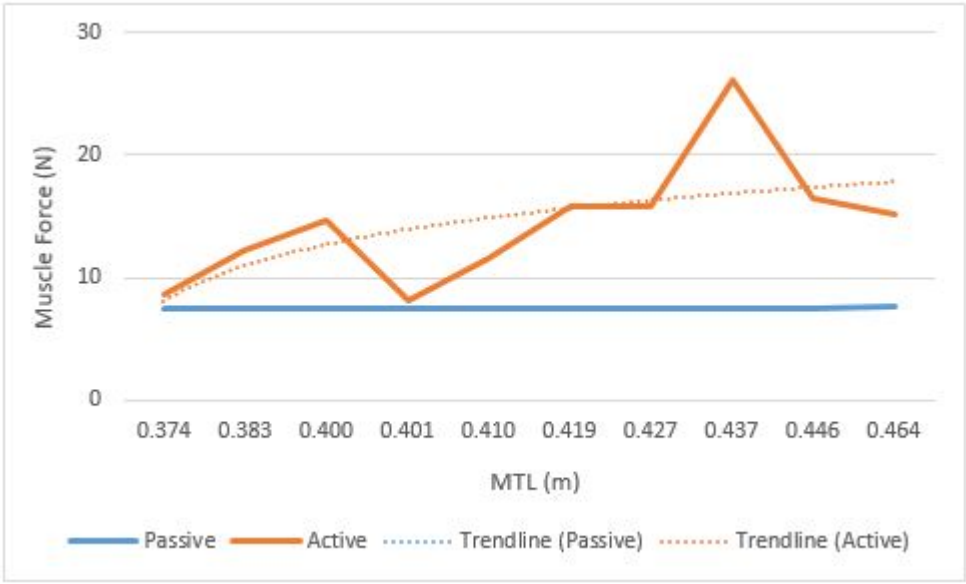

Figure 3.25 Limb 8 ST muscle-tendon complex length vs. muscle passive and active forces.

3.2.9 Patient 6 - Limb 9

Based on the gait cycle of the Limb 9 that belongs to the Patient 6, it can be seen that the gait relevant cycle starts with 0.17 seconds and this relevance vanishes after the 3.78 seconds. Four times repeating pattern can be observed for this limb

on the Figure 3.26, related to the both GRA and ST muscles. Similar to the other limbs and patients analyzed in this study, ST muscle-tendon complex length maximum values are relatively higher that GRA muscle maximum tendon length values.

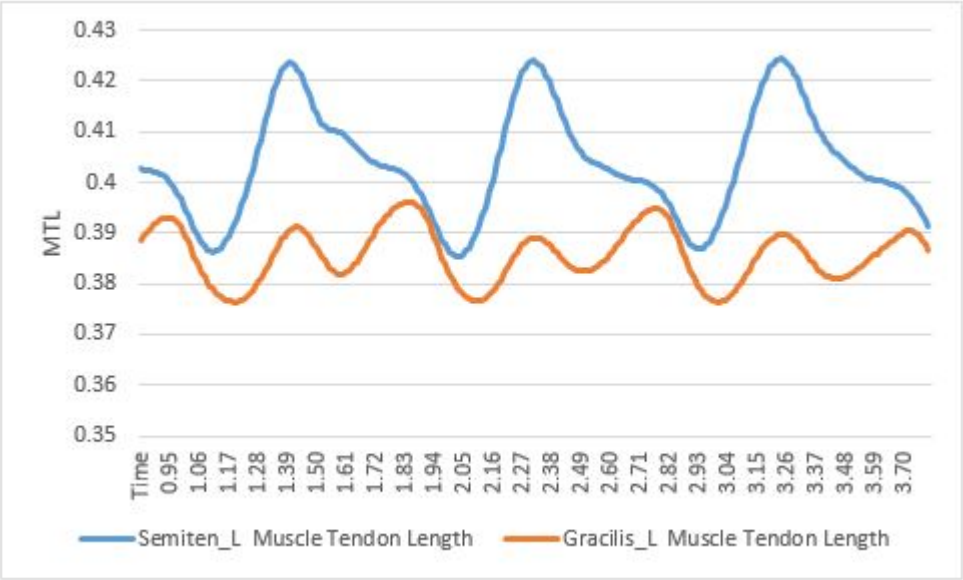

Figure 3.26 Limb 9 GRA and ST muscle-tendon complex length changes during the gait cycle.

Table 3.9 shows the muscle-tendon complex length and muscle force values for ten different data points. Same as the Patient 1 and Patient 3 whose both two limbs are studied via OpenSim simulations, the same muscle-tendon complex length values could be received for the two different limbs (Limb 8 and Limb 9) of Patient 6 as well. One single point on the list with 20° hip angle and 30° knee angle could be observed during the real gait cycle of the patient.

The GRA muscle passive force is stable with the increasing muscle-tendon complex length consistently. There is no important deviance on the graph of Figure 3.27. The active muscle force has a tendency to increase with the increasing muscle-tendon complex length despite some fluctuations.

Similar to the GRA muscle, ST muscle passive force values does not change significantly against the muscle-tendon complex length, as expected. The graph stayed almost straight for the entire muscle-tendon complex length values. The active ST

Table 3.9
Muscle-tendon complex length and muscle force data of Limb 9 for different hip and knee angles.

		GRA			ST		
HA	KA	Cond I (N)	Cond II (N)	MTL (m)	Cond I (N)	Cond II (N)	MTL (m)
45	120	6.299	18.680	0.361	8.685	11.790	0.401
45	90	5.919	53.450	0.372	8.753	35.330	0.41
45	60	6.619	63.650	0.387	8.811	35.940	0.427
45	30	7.729	63.550	0.402	8.758	34.210	0.446
45	0	12.499	65.370	0.414	9.253	19.440	0.464
20	120	5.549	14.700	0.349	8.715	9.340	0.374
20	90	5.659	53.710	0.36	8.742	20.900	0.383
20	60	5.939	69.130	0.376	8.790	37.060	0.4
20	30	6.499	68.680	0.39	8.833	39.990	0.419
20	0	12.319	59.220	0.402	8.887	45.760	0.437

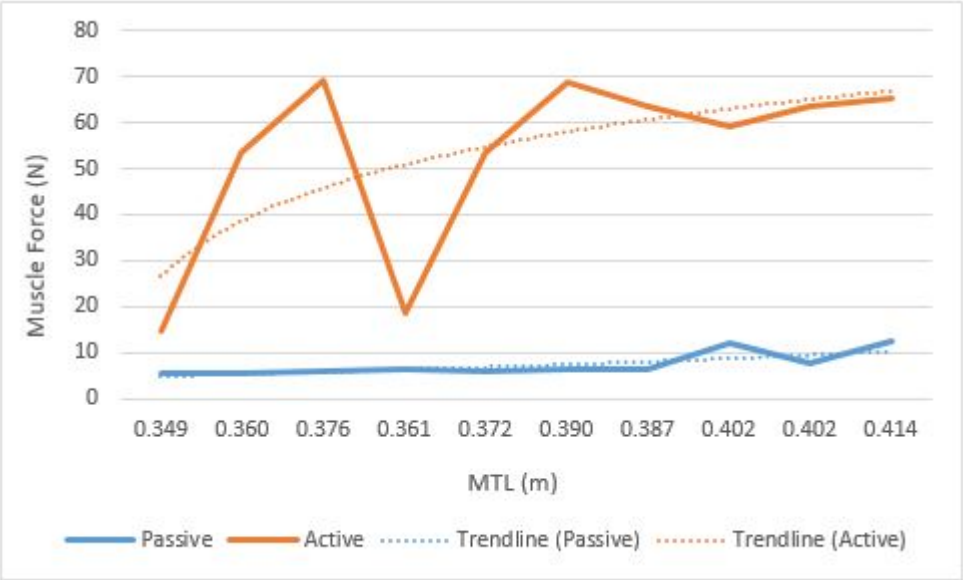

Figure 3.27 Limb 9 GRA muscle-tendon complex length vs. muscle passive and active forces.

muscle force behaved highly inconsistently as the Figure 3.28 contains lots of sharp deviances. However, the trendline shows a tendency to increase for active muscle force as well, against the increasing muscle-tendon complex length.

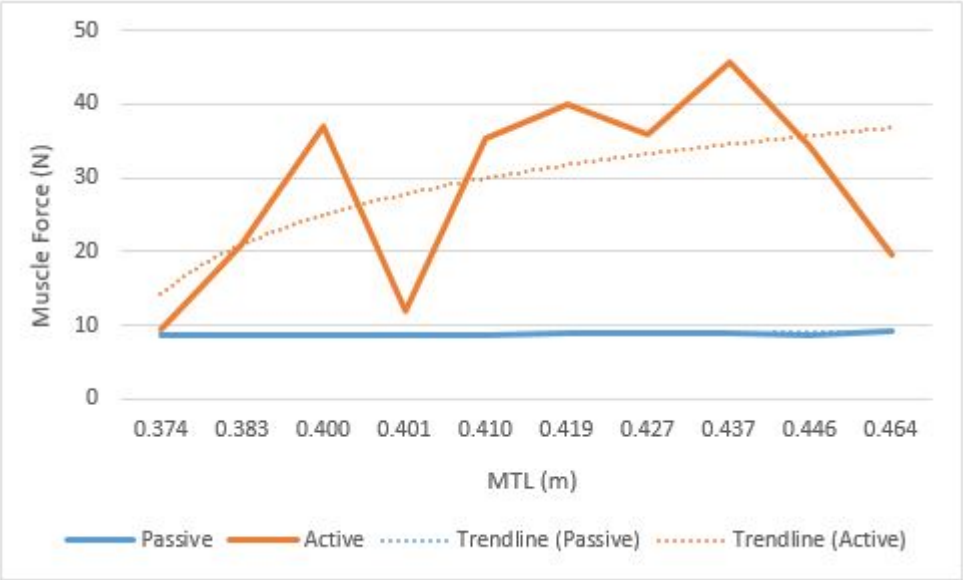

Figure 3.28 Limb 9 ST muscle-tendon complex length vs. muscle passive and active forces.

3.2.10 Patient 7 - Limb 10

Figure 3.29 contains the changing trends of GRA and ST muscle-tendon complex lengths during the gait cycle. It could be observed that both two muscles were persistent on their actions with three repeating patterns between the gait relevant time zones of 0.50 seconds and 2.88 seconds. Consistent with the other findings, ST muscle-tendon complex length values are higher compared to the GRA muscle values.

Table 3.10 shows the ten data points for muscle-tendon complex length and muscle force values for GRA and ST muscles of Limb 10. Three different points within this list could be seen on the gait cycle of the patient with the 0°- 30°- 60° knee angles with the constant hip angle of 20° for each.

Dissimilar to the other limbs in this study, GRA muscle passive and active force values are highly close to each other in general. This unexpected behavior could be seen on the Figure 3.30. Apart from this distinctness, GRA passive force can be said to decrease for most of the graph against the increasing muscle-tendon complex length while the active force has a tendency to increase in general when the trendline of the

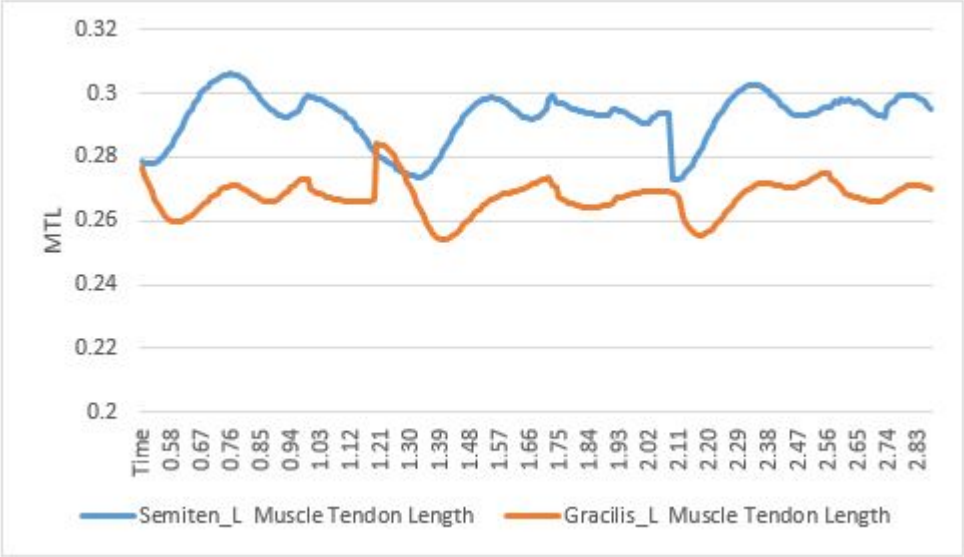

Figure 3.29 Limb 10 GRA and ST muscle-tendon complex length changes during the gait cycle.

Table 3.10
Muscle-tendon complex length and muscle force data of Limb 10 for different hip and knee angles.

		GRA			ST		
HA	KA	Cond I (N)	Cond II (N)	MTL (m)	Cond I (N)	Cond II (N)	MTL (m)
45	120	36.932	16.280	0.246	0	28.350	0.282
45	90	34.276	23.960	0.255	7.429	37.330	0.289
45	60	33.289	43.360	0.268	7.321	18.170	0.303
45	30	26.236	43.280	0.28	9.449	25.280	0.319
45	0	5.382	56.800	0.29	23.590	22.500	0.334
20	120	36.589	17.610	0.235	4.969	27.050	0.258
20	90	37.869	35.940	0.245	4.879	14.840	0.265
20	60	37.139	48.590	0.258	5.179	21.690	0.279
20	30	32.249	51.330	0.27	6.289	13.300	0.295
20	0	14.569	53.030	0.279	13.869	6.560	0.31

graph is studied.

The passive ST muscle force can be said to tend to increase against the increasing muscle-tendon complex length. The active muscle force behaved quite ambivalently with lots of high slope increasing and decreasing force trends. On the Figure 3.31, it can be said that the trendline shows decreasing characteristics for the active muscle force indifferent to the other spastic ST muscles. The starting and ending muscle active force points on the graph are lose to each other despite these tight turns.

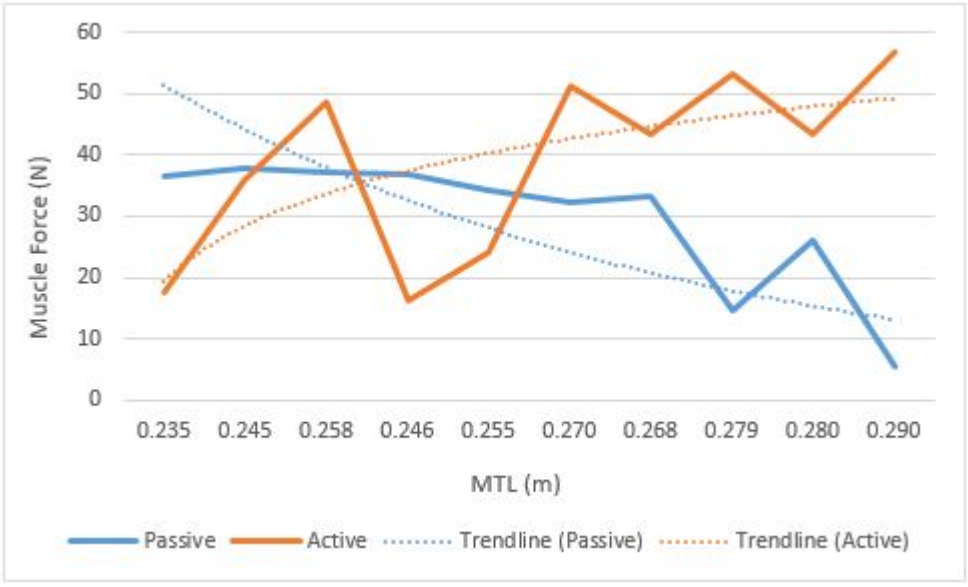

Figure 3.30 Limb 10 GRA muscle-tendon complex length vs. muscle passive and active forces.

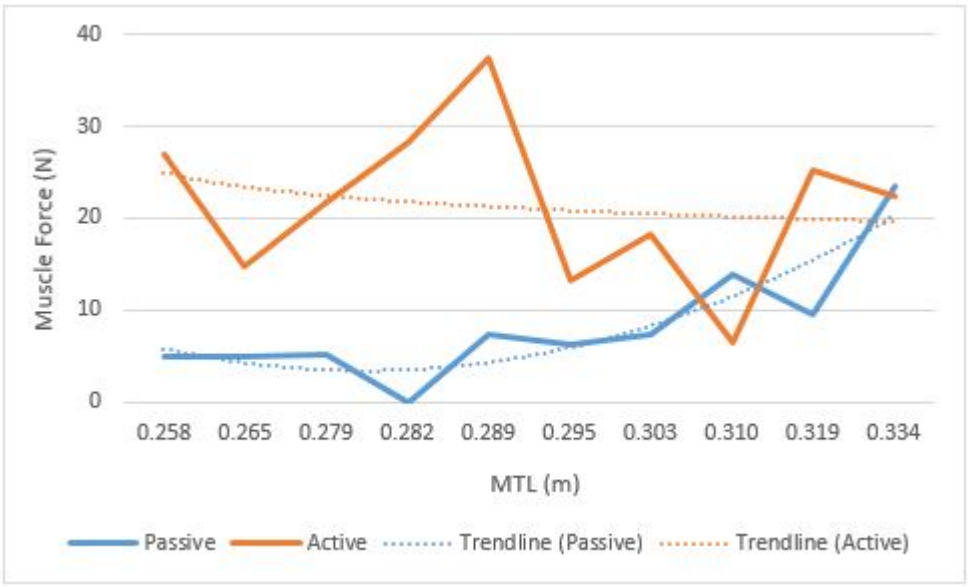

Figure 3.31 Limb 10 ST muscle-tendon complex length vs. muscle passive and active forces.

4. DISCUSSION AND CONCLUSION

The OpenSim simulations developed specifically for each patient and limb provided the analysis of muscle tendon unit length for both GRA and ST muscles. Figure 4.1 shows the change of normalized muscle-tendon complex length values for ten different limbs. For ST and GRA, the changes can be calculated as 9.9% +/- 2.2% and 6.8% +/- 1.7% respectively, and it can be concluded that the highest length values could be seen on the final part of the cycle.

Typically; the increasing muscle tendon unit length, which represents the extension of the knee, comes up with the mainly steady passive force curve for both GRA and ST but this almost steady curve ends with an increase in the passive force most of the time, at the end of the cycle. Another finding can be stated that these passive muscle forces are generally lower than the active forces for both GRA and ST muscles. Although the behavior of active muscle forces are not as consistent as passive forces, it can be deducted that there is a tendency to increase for them along with the increasing muscle-tendon complex length. For almost every case, the lowest active muscle force values were recorded with the minimum muscle-tendon complex length values. However, the number of several increasing and decreasing force trends seen on the graphs prevents to gain the direct and solid correlation between active muscle force and muscle-tendon complex length. All in all, even this kind of an implicit function between the muscle force and length could be acquired with this study for the very first time.

The previous studies suggested that maximum muscle force is seen at shorter muscle-tendon complex length, and total muscle force tends to decrease with the high muscle-tendon complex length. Besides, it is expected to observe from previous studies that active and muscle force values get closer to each other with the increasing muscle-tendon complex length. However, the muscle forces tended to increase in general in this study and active muscle forces stayed as the dominant agent. This situation for

the spastic muscles implies that some mechanical characteristics of the spastic muscles may behave similar to the healthy muscles in some manner.

The OpenSim model study assisted to obtain a platform containing the intraoperative mechanical tests and patient gait cycles. This kind of a platform is very useful for comparing the mechanical and clinical data for the best treatment method. An important finding showed that the muscle-tendon complex length changes are similar for healthy and spastic muscles, for both GRA and ST. Both the healthy and spastic GRA and ST muscles showed the minimum muscle-tendon complex length values in the beginning of the oscillation and the maximum values in the final part. Thus, muscle tendon unit length data cannot explain the exaggerated knee flexion and foot movement disorder that may be observed in the clinic during the initial loading and final discharge phases of gait cycles, contrary to the expectation that spastic muscles are relatively shorter. On the other hand, it should be noted that it is not possible to determine the existence of a shortened muscle body length that can explain the pathology. However, the fact that intraoperative muscle force measurements exhibited maximum muscle force at extension, which means long muscle tendon unit lengths, suggests that the bodies of spastic muscles may not be shortened compared to the healthy limbs.

Maximum passive force for ST and GRA occur when the target muscle is at the highest length. In gait related muscle tendon unit lengths, active forces are the dominant component of the total tendon forces of the respective muscles. It suggests that the limitations of joint movement clearly observed during gait in cerebral palsy patients are associated with active condition muscle force, not passive. However, the general force generating characteristics of the muscles are consistent with those of the healthy muscle, suggesting that individual spastic muscles may not be the determinant of joint movement limitations. This limiting effect may be enhanced by the simultaneous activation of the muscles.

OpenSim models assume that the muscles are mechanically fully isolated from each other, which ignores the possible effect of other co-activated muscles on the force

of the target muscle. Consequently, the phenomenon called epimuscular myofascial force transmission was ignored in the present study. However, it can still be considered that this study blazed a trail to adapt the gait analysis data into a model developed and can be improved by adding the epimuscular myofascial force transmission effects in the subsequent studies as OpenSim is open-source software.

In conclusion, using the model developed, this study enabled us to convert the intraoperatively measured knee joint angle-muscle force data into muscle-tendon complex length-muscle force data in patients with CP. The outcome of this assessment suggests that mechanical characteristics of spastic muscles may not necessarily differ from those of healthy muscles. This implies that, an explanation for the restricted joint movement of CP patients via the consideration of spastic muscles as shortened and mechanically abnormal muscles is a simplistic one.

REFERENCES

1. Gracies, J., "Pathophysiology of spastic paresis. i: Paresis and soft tissue changes," *Muscle and Nerve*, Vol. 31, no. 5, pp. 535–551, 2005.

2. Gracies, J., "Pathophysiology of spastic paresis. ii: emergence of muscle overactivity," *Muscle and Nerve*, Vol. 31, no. 5, pp. 552–571, 2005.

3. Botte, M., "Spasticity and contracture. physiologic aspects of formation," *Clinical Orthopaedics and Related Research*, Vol. 233, pp. 7–18, 1988.

4. O'Dwyer, N., "Reduction of spasticity in cerebral palsy using feedback of the tonic stretch reflex: a controlled study," *Developmental Medicine and Child Neurology*, Vol. 36, no. 9, pp. 770–786, 1994.

5. Farmer, S., "Contractures in orthopaedic and neurological conditions: a review of causes and treatment," *Disability and Rehabilitation*, Vol. 23, no. 13, pp. 549–558, 2001.

6. Tardieu, G., "Muscle hypoextensibility in children with cerebral palsy: Ii. therapeutic implications," *Archives of Physical Medicine and Rehabilitation*, Vol. 63, no. 3, pp. 103–107, 1982.

7. Brown, J., "Neurophysiology of lower-limb function in hemiplegic children," *Developmental Medicine and Child Neurology*, Vol. 33, no. 12, pp. 1037–1047, 1991.

8. Mirbagheri, M., "Intrinsic and reflex stiffness in normal and spastic, spinal cord injured subjects," *Experimental Brain Research*, Vol. 141, no. 4, pp. 446–459, 2001.

9. O'Dwyer, N., "Reflex hyperexcitability and muscle contracture in relation to spastic hypertonia," *Current Opinion in Neurology*, Vol. 9, no. 6, pp. 451–455, 1996.

10. Cortes, N., "Cerebral palsy group," 2016. https://cerebralpalsygroup.com/cerebral-palsy/.

11. Fergusson, D., "The epidemiology of major joint contractures: a systematic review of the literature," *Clinical Orthopaedics and Related Research*, Vol. 456, pp. 22–29, 2007.

12. Shortland, A., "Architecture of the medial gastrocnemius in children with spastic diplegia," *Developmental Medicine and Child Neurology*, Vol. 44, no. 3, pp. 158–163, 2002.

13. Kreulen, M., "Assessment of flexor carpi ulnaris function for tendon transfer surgery," *Journal of Biomechanics*, Vol. 41, pp. 2130–2135, 2008.

14. Smeulders, M., "Overstretching of sarcomeres may not cause cerebral palsy muscle contracture," *Journal of Orthopaedic Research*, Vol. 22, pp. 1331–1335, 2004.

15. Smith, L., "Hamstring contractures in children with spastic cerebral palsy result from a stiffer extracellular matrix and increased in vivo sarcomere length," *The Journal of Physiology*, Vol. 589, pp. 2625–2639, 2011.

16. Haberfehlner, H., "Assessment of net knee moment-angle characteristics by instrumented hand-held dynamometry in children with spastic cerebral palsy and typically developing children," *The Journal of Neural Engineering*, 2015.

17. Crenna, P., "Spasticity and 'spastic' gait in children with cerebral palsy," *Neuroscience and Biobehavioral Reviews*, Vol. 22, pp. 571–578, 1998.

18. Damiano, D., "Relationship of spasticity to knee angular velocity and motion during gait in cerebral palsy," *Gait and Posture*, Vol. 23, pp. 1–8, 2006.

19. Ada, L., "Does spasticity contribute to walking dysfunction after stroke?," *Journal of Neurology, Neurosurgery, and Psychiatry*, Vol. 64, p. 628, 1998.

20. Norton, B., "Correlation between gait speed and spasticity at the knee," *Physical Therapy*, Vol. 55, pp. 355–359, 1975.

21. Yucesoy, C., "Epimuscular myofascial force transmission implies novel principles for muscular mechanics," *Exercise and Sport Sciences Reviews*, Vol. 38, pp. 128–134, 2010.

22. Ates, F., "Muscle lengthening surgery causes differential acute mechanical effects in both targeted and non-targeted synergistic muscles," *Journal of Electromyography and Kinesiology*, Vol. 23, pp. 1199–1205, 2013.

23. Ates, F., "The mechanics of activated semitendinosus are not representative of the pathological knee joint condition of children with cerebral palsy," *Journal of Electromyography and Kinesiology*, Vol. 28, pp. 130–136, 2016.

24. Yucesoy, C., "Intra-operatively measured spastic semimem-branosus forces of children with cerebral palsy," *Journal of Electromyography and Kinesiology*, Vol. 36, pp. 49–55, 2017.

25. Davis, R., "A gait analysis data collection and reduction technique," *Human Movement Science*, Vol. 10, pp. 575–587, 1991.

26. Kaya, C., "Intraoperative experiments combined with gait analyses indicate that active state rather than passive dominates the spastic gracilis muscle's joint movement limiting effect in cerebral palsy," *Clinical Biomechanics*, Vol. 68, pp. 151–157, 2019.

27. Delp, S., "Opensim: Open-source software to create and analyze dynamic simulations of movement," *IEEE Transactions on Biomedical Engineering*, Vol. 55, pp. 1940–1950, 2007. https://simtk.org.

28. Seth, A., "Opensim: Simulating musculoskeletal dynamics and neuromuscular control to study human and animal movement," *PLOS Computational Biology*, Vol. 14, no. 7, 2018.

29. Barre, A., "Mokka motion kinematic and kinetic analyzer," 2011. https://biomechanical-toolkit.github.io/mokka/.